

# Proton fluctuations and water diffusion in dextran chemical hydrogels studied by incoherent elastic and quasielastic neutron scattering

Gaio Paradossi,\* Francesea Cavalieri and Ester Chiessi

*Dipartimento di Chimica, Università di Roma Tor Vergata and INFM, via della Ricerca Scientifica, 00133 Roma, Italy*

Received 14 September 2004; accepted 31 December 2004

Dedicated to Professor David A. Brant

**Abstract**—Proton fluctuations reporting local motions of the glycosidic linkages of chemically crosslinked dextran hydrogels with well defined pore-size distribution are studied by static and dynamic neutron scattering approaches. The dependence of the dynamic behaviour of water on the pore sizes is also discussed.

© 2005 Elsevier Ltd. All rights reserved.

**Keywords:** Neutron scattering; Dextran hydrogels; Water diffusion

## 1. Introduction

The dynamic behaviour of polymeric hydrogels has been the subject of several investigations, including progressively new and more-complex macromolecular systems. An understanding at the molecular level of the dynamics of the hydrogel components constitutes basic information for the formulation of new platforms for drug delivery with complex time-window patterns, such as controlled or pulsed release.<sup>1,2</sup> In this respect, polysaccharides are a promising component in the design of soft condensed-matter devices for biomedical applications.<sup>3</sup> Networks based on this class of macromolecule offer several advantages, such as biocompatibility, and the possibility of controlled degradation, employing physical or chemical crosslinking. The experimental observation of such molecular parameters as the microscopic solvent diffusion dynamics or the local displacement fluctuations of polymer chains in gels are often complicated by the structural heterogeneity of the network studied,<sup>4</sup> averaging out the results that can be used for establishing a relationship between structure and dynamic properties. In this context we have studied the

dynamics at the microscopic level of a series of chemically crosslinked dextrans having narrow (monodisperse) pore-size distribution. Such hydrophilic networks, known as Sephadexes, are used as packing materials in gel-permeation chromatography (GPC). We have used Sephadex samples as model systems for studying the dynamics of the polysaccharide chains and diffusion of water over a wide range of pore sizes. The wide range of scattering vectors and of energies now available in high-flux neutron facilities permit the study of molecularly localized diffusive motions, with characteristic times ranging from a few nanoseconds to a few picoseconds, a dynamic range where it is now possible to compare the experimental findings with molecular-dynamics simulations.

The pore sizes of different types of Sephadex were evaluated by studying their equilibrium swelling behaviour.<sup>5</sup> Successive experiments were carried out at the ISIS<sup>6</sup> and ILL<sup>7</sup> neutron facilities for elastic and quasielastic incoherent neutron scattering. The elastic experiment studied the structural fluctuations of the polysaccharide chains constituting the network whereas the quasielastic measurements addressed the dynamics of the solvent. This study is part of a larger program on the dynamic processes occurring in soft condensed-matter devices for biomedical applications; it concerns

\* Corresponding author. E-mail: [paradossi@stc.uniroma2.it](mailto:paradossi@stc.uniroma2.it)

the dynamics of the two components in the hydrogels, namely the polysaccharide and water. Due to the characteristics of the probing particles (neutrons), the results concern the motions of hydrogen atoms, as their large incoherent cross-sections and their abundance in carbohydrate hydrogels constitute the major contribution to the measured neutron-scattering intensity.<sup>8</sup>

Incoherent elastic neutron scattering allows an approach to the local structural fluctuations of the polymer moiety by examining deviations of the elastic scattering law,<sup>8</sup>  $S(q, 0)$ , from Gaussian behaviour as a function of the temperature<sup>9</sup> in terms of a two-well potential model (Eq. 1).<sup>10</sup> This analysis yields a distance,  $d$ , separating the wells and the occupation probabilities of the two sites,  $p_1$  and  $p_2$ .

$$S(q, 0) = \exp[-2W(q)] \left\{ 1 - 2p_1p_2 \left[ 1 - \frac{\sin(qd)}{(qd)} \right] \right\} + bkg \quad (1)$$

where the exponential first term is the Debye–Waller factor with  $W(q)$  describing the Gaussian contribution to the hydrogen atoms mean-square displacement,<sup>9</sup>  $\langle \Delta u^2 \rangle_G$ , namely  $W(q) = q^2 \langle \Delta u^2 \rangle_G / 6$ . With this simplified model it is possible to extract information about the structural fluctuations of the hydrogens bound to the matrix.

Deuterated water is often used if the focus is on the scattering behaviour of the polymer moiety. However, this procedure assumes that substitution of water by deuterated water does not influence the structural and dynamic behaviour of the polysaccharide network. This matter has been discussed in the literature,<sup>12,13</sup> reporting remarkable differences in terms of solvation properties and conformational state of the protein solute in the two solvents. For this reason we have chosen water as solvent, to avoid influence by deuterated solvent on the structure and local dynamics of the polysaccharide network. Possible contributions, deriving from hydrogens of the diffusing molecules of water to the elastic  $S(q, 0)$  function have been already addressed.<sup>13,14</sup> As the energy and momentum resolutions of the spectrometer used for this study (IN13 at ILL) are 8  $\mu\text{eV}$  and 1  $\text{\AA}^{-1}$ , respectively, these features imply that only molecules able to span 1  $\text{\AA}$  in 0.1 ns will contribute to the  $S(q, 0)$  term. In this respect, the contribution of bulk water possibly present in our samples (see Section ‘Water dynamics’), is negligible as the reported value of diffusion coefficient for bulk water at 25  $^\circ\text{C}$  is  $2.5 \times 10^{-5} \text{ cm}^2 \text{ s}^{-1}$ .<sup>15</sup> However, because of the interaction with the polysaccharide moiety, the presence of water molecules with slowed diffusivity may contribute to the elastic scattered intensity. We have evaluated<sup>14</sup> this contribution on the basis of data provided by incoherent quasielastic neutron scattering (QENS) experiments carried out in parallel on the IRIS facility at ISIS, Didcot, UK. This study showed that

the slowly diffusing fraction of water molecules has a diffusion coefficient ranging from  $0.5 \times 10^{-5}$  to  $1.5 \times 10^{-5} \text{ cm}^2 \text{ s}^{-1}$ , thus contributing to the overall elastic scattering as a flat background, as indicated in Eq. 1. Moreover, from the quasielastic measurements carried out at ISIS, the microscopic dynamics of the solvent has been determined on Sephadex samples.

The main goal of this study is to establish a correlation between the dynamic behaviour of hydrogel components and porosity of matrixes with well defined mesh-size distribution, to permit a better understanding of the molecular dynamic properties of novel matrices and help the design of hydrogels with controlled diffusional features.

## 2. Experimental

### 2.1. Samples

Sephadex G10, G15, G50, G75 and G100 samples were purchased from Pharmacia and were combined with double distilled water up to a fixed  $\text{H}_2\text{O}$  content of 60% (w/w) for elastic and quasielastic neutron-scattering experiments. The wet samples were equilibrated overnight in capped containers.

### 2.2. Maximum swelling degree and pore-size determinations

The equilibrium water content of Sephadex samples was determined by using an aqueous solution of Blue Dextran at a concentration of 6 mg/mL according the method validated by Stenekes and Hennink<sup>16</sup> based on the exclusion of a high-molecular-weight compound. Known amounts of dry samples were rapidly hydrated over few minutes and the swollen microspheres were separated from solution by centrifugation. As the overall dimensions of Blue Dextran do not allow permeation of the polysaccharide hydrogel, the increase in Blue Dextran concentration in the supernatant was readily quantified spectrophotometrically at  $\lambda = 610 \text{ nm}$ . The measured water uptake was converted into the polymer volume fraction,  $\phi_2$ , and the molecular weight between two crosslinks,  $M_c$ , was obtained by means of the Flory–Rehner theory<sup>17</sup> and corrected, for the higher crosslinking density samples, by non-Gaussian chain behaviour (Eq. 2).<sup>18</sup>

$$\frac{1}{M_c} = - \left( \frac{1}{\rho_2 v_1} \right) \cdot \frac{\{ \ln(1 - \phi_2) + \phi_2 + \chi_1 \phi_2^2 \}}{\{ \phi_2^{1/3} - \frac{1}{2} \phi_2 \}} \cdot \frac{\left[ 1 - \frac{\phi_2^{2/3}}{N} \right]^3}{\left[ 1 + \frac{\phi_2^{1/3}}{N} \right]^2} \quad (2)$$

where  $\rho_2$  is the density of dextran and  $\chi_1$  is the Flory–Huggins interaction parameter equal to 0.496 for the dextran–water system,<sup>19</sup>  $v_1$  is the molar volume of water and  $N$  is the number of repeating units between crosslinks.

### 2.3. Neutron-scattering experiments

Incoherent elastic neutron-scattering measurements were carried out at the backscattering spectrometer IN13<sup>11</sup> at the ILL facility. The instrumental resolution of 8  $\mu\text{eV}$  (full width at half maximum, FWHM) was determined by calibrating the instrument with vanadium. The temperatures explored ranged from 275 to 320 K. Data were corrected for the absorption and normalized with respect to vanadium scattering, using the software package ELASCAN available at ILL. Data were analyzed in terms of Eq. 1.

QENS experiments were carried out at the ISIS pulsed neutron facility (Rutherford Appleton Laboratory, Chilton, UK) using the time-of-flight inverted-geometry backscattering spectrometer IRIS<sup>20</sup> in the PG 002 configuration. Under these conditions the FWHM resolution was 15  $\mu\text{eV}$ . The double differential incoherent cross-section was measured over an energy window,  $\Delta\omega$ , ranging from  $-0.4$  to  $0.9$  meV and over a scattering vector,  $q$ , from  $0.44$  to  $1.84$   $\text{\AA}^{-1}$ . Raw data were corrected for absorption and detector efficiencies and normalized using the standard software package GUIDE available from ISIS.

Aluminium flat cells of  $0.02$  cm thickness were used for all measurements, and corrections for multiple scattering were not applied. Samples were weighed before and after measurements. Variations within 10% were observed.

The instrumental resolution,  $R(\omega)$ , determined by running a vanadium slab is convoluted with a trial  $S_{\text{inc}}(q, \omega)$  model function:<sup>21</sup>

$$S_{\text{inc}}(q, \omega) = \frac{1}{A} \{ p[A_0(q)\delta(\omega) + (1 - A_0)L_p(q, \omega)] + (1 - p)[w_S L_S(q, \omega) + (1 - w_S) \times L_F(q, \omega)] \} + BL \quad (3)$$

In Eq. 3,  $A$  is a normalization factor,  $p$  and  $w_S$  are the molar fractions of the polymer moiety and of the slow relaxing water,  $A_0$  is the fraction of elastic intensity due to the polymer moiety over the total intensity. The dynamics of the polymer and water are described in Eq. 3 by means of three Lorentzian terms  $L_p$ ,  $L_S$  and  $L_F$ , respectively.

A minimization procedure with respect to the experimental scattering function,  $S_{\text{inc}}^{\text{exp}}(q, \omega)$ , yields the parameters of interest. In particular the half widths at half maximum (HWHM) of the  $L_p$ ,  $L_S$  and  $L_F$  are informative for the dynamic patterns of the moieties constituting the gel phase.

### 3. Results and discussion

Chemical and physical hydrogels display intrinsic micro-heterogeneities upon swelling. In the swollen state, due to the uneven distribution of junction zones in the network volume, there will be domains in the proximity of the crosslinking points with higher chain density. In the lower chain-density regions, chains will be dynamically and structurally more loose, and able to accommodate a larger quantity of water. The use of matrixes with practically monodisperse pore-size distributions permits the study of structural and dynamic properties of the polymer moiety and of the solvent contained in the networks. Characterization of the pore sizes of different polysaccharide networks was obtained by measuring the polymer volume fractions at the maximum swelling, and converting these observations into the corresponding value of molecular weight between crosslinks,  $M_c$ , by means of standard Flory–Rehner theory. In Table 1 the  $M_c$  values for the networks studied in this work are reported together with the correlation length,  $\xi$ , between crosslinks (see Eq. 4)<sup>18</sup> treating dextran chains as semiflexible and having characteristic ratio,  $C_n$ , of 1.8,<sup>22</sup> where  $l$  and  $M_0$  are the length and the molecular weight of the repeating unit, respectively.

$$\xi = \phi_2^{-1/3} \left( C_n \frac{2M_c}{M_0} \right)^{1/2} l \quad (4)$$

This parameter can be related to a characteristic linear pore dimension, which in the investigated samples spans from about  $10$   $\text{\AA}$  to  $\sim 100$  nm.

#### 3.1. Polymer chain fluctuations

Observation of the protons of the polymer network in the presence of water is possible with IN13, since the time–space resolution cancels out the contributions due to proton solvent as it was discussed in the introduction.

In our case, for  $q < 1.8$   $\text{\AA}^{-1}$ , Eq. 1 can be approximated to:<sup>9</sup>

$$S(q, 0) = \exp(-q^2 \langle u^2 \rangle / 3) \quad (5)$$

The semilogarithmic plot of  $S(q, 0)$  as a function of  $q^2$  in the low  $q$  region shown in Figure 1 for G15, G50 and G100 Sephadex samples is linear with

**Table 1.** Structural parameters of Sephadex hydrogels<sup>a,b</sup>

Sample	$\phi_2$	$M_c$ (g/mol)	$\xi$ ( $\text{\AA}$ )	$\xi$ ( $\text{\AA}$ ) at 60%
G10	0.56	370	16	16
G15	0.34	890	30	30
G50	0.095	35,000	290	200
G75	0.072	73,000	460	290
G100	0.052	170,000	790	440

<sup>a</sup> Parameters estimated assuming a Flory–Huggins constant  $\chi = 0.496$ .

<sup>b</sup> Errors within 10%.

slopes corresponding to the overall mean-square fluctuations of the hydrogen atoms of the polysaccharide chains.

These findings indicate that, at a degree of hydration of 60% (w/w), the smallest pore-size matrix ( $= 31 \text{ \AA}$ ) displays a reduced flexibility compared with the pore-size matrices of  $\sim 200$  and  $400 \text{ \AA}$  (see Table 1), in agreement with the macroscopic observations obtained from swelling measurements.

The analysis of  $S(q, 0)$ , based on a simplified two-well potential,<sup>10</sup> extended to the complete set of  $q$  values, provides additional information on the segmental displacement fluctuations of the saccharide chains. According to this model (Eq. 1), the proton fluctuations are described as random jumps between two sites, with a standard free-energy difference  $\Delta G^\circ$  and separated by a distance  $d$ .

A typical result of the fitting procedure of  $S(q, 0)$  as a function of  $q^2$  is shown in Figure 2.

The analysis carried out on the three hydrogels shows a constant value of  $d$  equal to  $3 \text{ \AA}$  between two states, independent of the porosities, and an equal occupation probabilities,  $p_1 = p_2 = 0.5$ , of finding a proton in one of the two states, indicating a negligible difference in the standard free energy of the two sites. Despite the approximate picture provided by this model, a connection to the structural features of the polysaccharide constituting these networks can be envisaged in the involvement of the  $\alpha$ -D-(1 $\rightarrow$ 6) saccharide linkage hydrogens, as suggested by experimental and conformational studies of this saccharide junction. A graphic support to this interpretation is shown in Figure 3.

In this context the conformational freedom of an  $\alpha$ -D-(1 $\rightarrow$ 6)-linked glucan was studied by Brant et al. by mea-

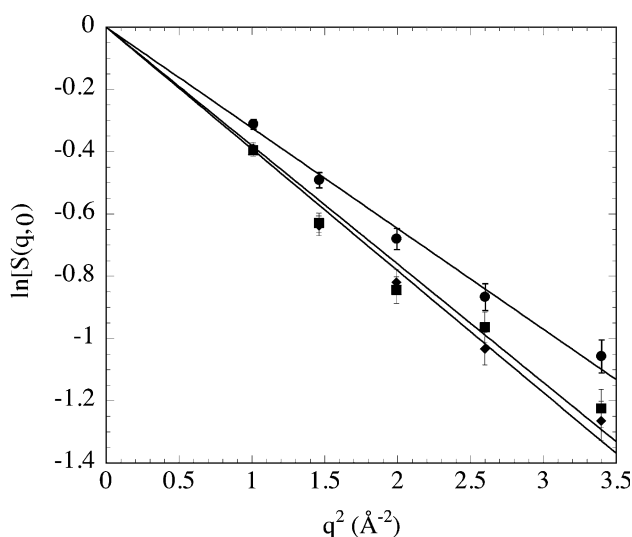


**Figure 1.** Semilogarithmic plot of the normalized incoherent elastic scattering function,  $S(q, 0)$ , for three different Sephadex samples as a function of the squared scattering vector for low  $q$  values. (●) G15; (■) G50; (◆) G100.

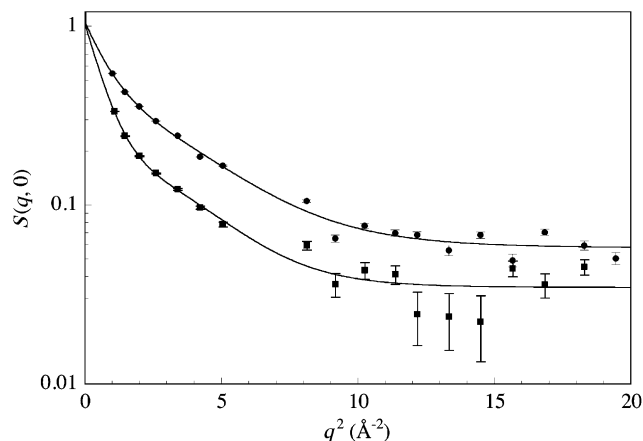


**Figure 2.** Normalized incoherent elastic scattering function,  $S(q, 0)$ , as a function of  $q^2$  for G15 at a degree of hydration of 60% (w/w) at 319 K (■) and at 275 K (●).

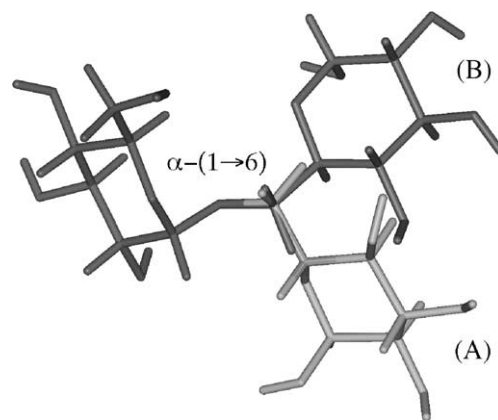


**Figure 3.**  $\alpha$ -(1 $\rightarrow$ 6) Dimeric segment in two conformations of minimum energy (A, B). The unlabelled sugar ring is common to both conformations.

surements of  $^{13}\text{C}$  NMR relaxation times,<sup>23</sup> sampling the rate of conformational changes and ultimately the dynamics of the single carbon atoms of the chains, using small-angle X-ray scattering and conformational analysis.<sup>24</sup> The main contribution to the overall chain flexibility of a polysaccharide is provided by the fluctuations of the torsional angles around the glycosidic linkages of the dextran.

### 3.2. Water dynamics

The dynamics of processes occurring in the hydrogel networks in the picoseconds range can be obtained by incoherent quasielastic neutron scattering. In hydrated polysaccharide systems, incoherent scattering of hydrogens dominates, as the proton cross-section is larger than that of the other nuclei typically contained in the samples. Therefore the observed incoherent dynamic scattering factor,  $S_{\text{inc}}(q, \omega)$ , mainly provides information

on the dynamics of hydrogens present in the gel. In this work, analysis of the broadening of the incoherent quasielastic scattering law allowed to study the dynamics of water on different Sephadex hydrogels, covering a pore size from few to hundreds of angstroms. Studies on the confinement of water in different hydrophilic networks<sup>25–28</sup> have shown that diffusive behaviour of water is strongly influenced by the presence of polar matrixes. In agarose and hyaluronic hydrogels, water microdynamics is influenced by the setting of a network of H-bonding sites, leading to an increase of the size of transient water clusters. In hydroxylated vinyl-polymer chemical hydrogels, the diffusion behaviour of water has been analyzed in terms of the model described by Eq. 3, and showed a combination of slowly diffusing water molecules and of a larger amount of water characterized by a diffusional behaviour much closer to bulk water.

For all Sephadex samples investigated, two dynamically different fractions of water are recognizable. The fast-relaxing water molecules, described in the model (Eq. 3) by a Lorentzian term,  $L_F$ , have a microscopic diffusional behaviour close that of bulk water, showing that even at a moderate degree of hydration, namely 60% (w/w), dextran matrices accommodates bulk water in the network meshes. Typically the analysis of the half width at half height,  $\Gamma_S$ , of the Lorentzian  $L_S$  (see Eq. 3) describing the microscopic dynamics of the ‘slow’ molecules of water is performed in terms of restricted jump-diffusion models. This interpretative scheme describes the diffusion of a liquid in terms of residence sites separated by a diffusion event called ‘jump’. Simplified equations are obtained in the approximation of a much smaller ‘jump’ time compared to the time spent by the particle in a residence state. The residence time,  $\tau$ , and the jump length,  $h$ , can be obtained as fitting parameters of the dependence of the broadening factors on the scattering vector values. From these parameters a microscopic diffusion coefficient,  $D$ , can be obtained by means of the relation  $D = \frac{h^2}{6\tau}$ .

As probed distances get shorter, that is, at the larger scattering vectors, the broadening factor,  $\Gamma_S$ , deviates from the continuous (Fickian) behaviour predicting a quadratic dependence on  $q$ . This feature has also been observed for bulk water,<sup>29</sup> indicating that a ‘long range’ correlation is present in this H-bonded liquid.

Confined water diffusion is often described by the Singwi–Sjölander jump-diffusion model, or random jump model (Eq. 6)<sup>30</sup> and the Chudley–Elliott model,<sup>31</sup> a diffusion model with fixed jump length (Eq. 7):

$$\tau\Gamma_S = \frac{(qh)^2}{6 + (qh)^2} \quad (6)$$

$$\tau\Gamma_S = [1 - \sin(qh)/(qh)] \quad (7)$$

In Figure 4 the behaviour predicted by these models are shown in comparison. The Chudley–Elliott model (Eq. 7) differs from the random-jump diffusion model at high  $q$ 's, where the broadening factor,  $\Gamma_S$ , shows an oscillatory trend converging to the asymptotic value shared with the random jump model (Eq. 6). The choice of model is made by comparison of the theoretical prediction with the experimental findings at high values of the scattering vector.

Investigations on polymer hydrogels have shown that the slowly diffusing entrapped water behaves as a supercooled liquid.<sup>27</sup> This diffusive behaviour is characterized by a longer residence time,  $\tau$ , compared to the values obtained for pure water at the same temperature. Moreover the dependence of and of the diffusion coefficient  $D$  on the temperature allows for an evaluation of the activation energy,  $E_a$ , necessary for promoting a jump. Typical values of  $E_a$  are found to be close to hydrogen bond energies.<sup>27,32</sup>

In the study of regularly spaced hydrogels as Sephadex, the dependence of the broadening factor,  $\Gamma_S$ , as a function of the scattering vector displays a trend indicating a well defined jump length (see Fig. 5).

Using Eq. 7 as fitting equation, a set of values of  $\tau$ ,  $h$  and  $D$ , as listed in Table 2, were obtained for different Sephadex samples.

Literature studies on hydrogels based on polysaccharides,<sup>25</sup> (hyaluronate and agarose), and on synthetic polymers as poly(vinyl alcohol)<sup>26,27</sup> are characterized by two water domains with different diffusion regimes. This is also observed for the Sephadex samples studied (see Eq. 3). However, in this case, a closer trend can be observed of the  $\Gamma_S$  value versus  $q$ , shown in Figure 5, to the behaviour predicted by the Chudley–Elliott model. This feature may be explained taking into account the substantial monodispersity of the pore-size

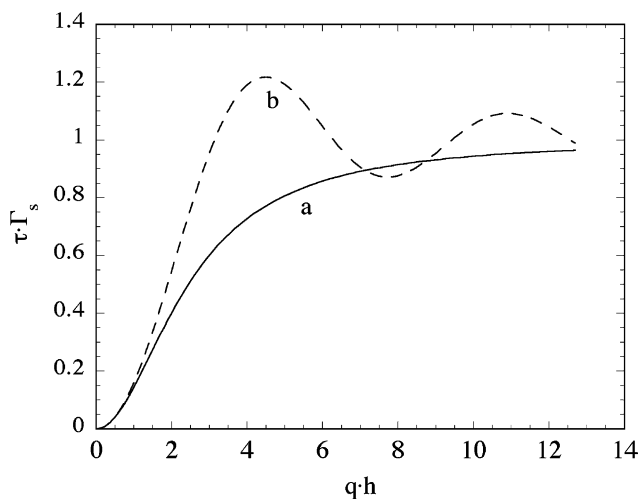


**Figure 4.** Reduced half width at half maximum,  $\Gamma_S$ , of the Lorentzian function,  $L_S$  (Eq. 3), as a function of reduced length for the random-jump model (Eq. 6, —) and Chudley–Elliott model (Eq. 7, ---).

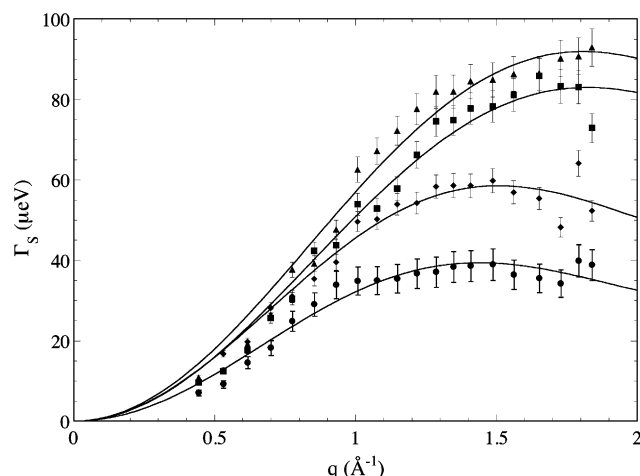


**Figure 5.** Half width at half maximum of the Lorentzian function,  $L_S$ , as a function of  $q$  at 30 °C for G10 (●), G50 (◆), G100 (■), G150 (▲). Fitting lines according to Eq. 7.

**Table 2.** Diffusion parameters of water ‘slow component’ according to Chudley–Elliott model (Eq. 7)

Sephadex	$\tau$ (ps)	$h$ (Å)	$D$ (cm <sup>2</sup> /s) $\times 10^5$
G10	$20.3 \pm 0.4$	$3.1 \pm 0.1$	$0.50 \pm 0.02$
G50	$13.7 \pm 0.2$	$2.9 \pm 0.1$	$1.08 \pm 0.04$
G100	$9.7 \pm 0.2$	$2.5 \pm 0.1$	$1.0 \pm 0.1$
G150	$8.7 \pm 0.2$	$2.5 \pm 0.1$	$1.2 \pm 0.1$

distribution characterizing these systems. The molecules of water in close interaction with the hydrophilic network, that is, the fraction of water molecules with slowed diffusion, diffuse according to more regular patterns as compared to the diffusion occurring in hydrogels characterized by highly polydisperse pore-size

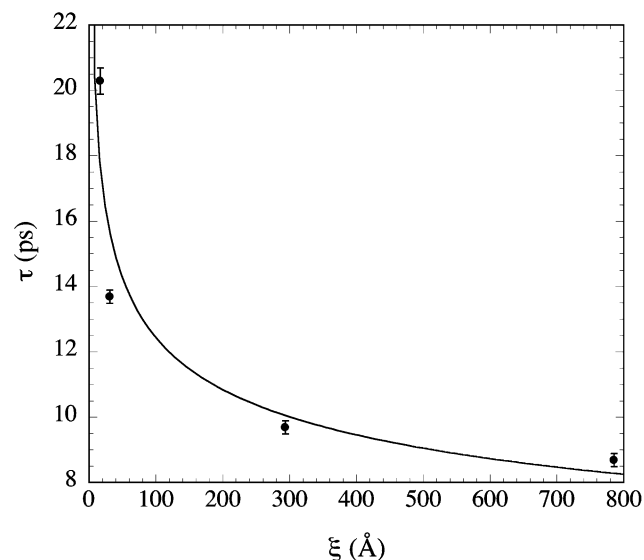


**Figure 6.** Residence time,  $\tau$ , according to Eq. 7, as a function of the network correlation distance,  $\xi$ , at 30 °C. The full line is a guide.

distributions. Although the jump lengths are not affected by the pore dimensions (since in all cases they are shorter than the pore sizes of the networks studied), the residence times listed in Table 2 are remarkably influenced by the structural features of the hydrogels. In Figure 6 the trend characterizing the residence-time dependence on pore size shows an asymptotic behaviour for large correlation length, that is, lower crosslinking density.

This finding indicates that the diffusion properties of the slowly diffusing water fraction is mainly influenced by the number of crosslinks encountered in the diffusion trajectories.

#### 4. Concluding remarks

Numerous dynamic processes occur in a polymer network, and many of them are coupled. A clear picture of the dynamic state of the components of a hydrogel is still a goal to achieve. This study offers a few points useful for further analysis:

1. Dynamic processes observed by QENS occur in time windows directly accessible to molecular dynamic calculations. Calculated microscopic diffusion parameters therefore can be compared to experimental ones for a complete description of the gel systems. In this respect molecular dynamics simulations on Sephadex hydrogels with different crosslinking densities allow formulation of a realistic description of a hydrogel at the molecular scale.
2. The residence times extracted from the QENS data depend on the hydrogel pore size in analogy with NMR relaxation times,  $T_1$  and  $T_2$ , observed under similar conditions.<sup>33,34</sup> In these papers the  $T_1$  and  $T_2$  behaviour as a function of the pore size of Sephadex (given in terms of the molecular weight exclusion limits of globular proteins) show a sharp increase of their values between G25 and G50 in agreement to our neutron-scattering approach (see Table 2). This correlation indicates that the dynamic processes observed on different time scales are both influenced by the structural features of the network.
3. The characteristic jump lengths of the constrained water fraction as found in this study, are similar to the mean fluctuation distances of the polysaccharide moiety, indicating the effective coupling of the two moieties.

#### Acknowledgements

This work was supported by MIUR (Grant 2004024358\_004).

## References

1. Breimer, D. D. *J. Controlled Release* **1999**, 62, 3–6.
2. Langer, R.; Tirrell, D. A. *Nature* **2004**, 428, 487–492.
3. Dumitriu, S.; Dumitriu, M. In *Polysaccharides in Medicinal Applications*; Dumitriu, S., Ed.; Marcel Dekker: New York, 1996; pp 705–764.
4. Shibayama, M. *Macromol. Chem. Phys.* **1998**, 199, 1–30.
5. Park, K.; Shalaby, W. S. W.; Park, H. In *Biodegradable Hydrogels for Drug Delivery*; Technomic: Lancaster, 1993; pp 67–98.
6. <http://www.isis.rl.ac.uk/>.
7. <http://www.ill.fr/>.
8. Bée, M. In *Quasielastic Neutron Scattering*; Adam Hilger: Bristol, 1988; pp 11–27.
9. Doster, W.; Cusak, S.; Petry, W. *Nature* **1989**, 337, 754–756.
10. Stoeckli, A.; Furrer, A.; Schoenenberger, C. H.; Meier, B. H.; Ernst, R. R.; Anderson, I. *Physica* **1986**, 136B, 161–164.
11. Deriu, A.; Paciaroni, A.; Zaccai, G.; Pfister, C. *Physica B* **2000**, 276, 512–513.
12. Nemethy, G.; Scheraga, H. *J. Chem. Phys.* **2002**, 41, 680–689.
13. Tehei, M.; Madern, D.; Pfister, C.; Zaccai, G. *Proc. Natl. Acad. Sci. U.S.A.* **2001**, 98, 14356–14361.
14. Paradossi, G.; Cavalieri, F.; Chiessi, E.; Mondelli, C.; Telling, M. T. F. *Chem. Phys.* **2004**, 302, 143–148.
15. Krynicki, K.; Green, C. D.; Sawyer, D. W. *Faraday Discuss. Chem. Soc.* **1978**, 66, 199–208.
16. Stenekes, R. J. H.; Hennink, W. E. *Int. J. Pharm.* **1999**, 189, 131–135.
17. Flory, P. J.; Rehner, R. *J. Chem. Phys.* **1943**, 11, 521–526.
18. Peppas, N. A.; Barr-Howell, B. D. In *Hydrogels in Medicine and Pharmacy*; Peppas, N. A., Ed.; CRC: Boca Raton, 1986; pp 28–34.
19. Schuld, N.; Wolf, B. A. In *Polymer Handbook*; Brandrup, J., Immergut, E. H., Grulke, E. A., Eds.; Wiley and Sons: New York, 1999; pp VII-247–VII-264.
20. Telling, M. T. F.; Campbell, S. I.; Abbley, D. D.; Cragg, D. A.; Balchin, J. J. P.; Carlile, C. J. *Appl. Phys. A* **2002**, 74, s61–s68.
21. Paradossi, G.; Cavalieri, F.; Chiessi, E.; Telling, M. T. F. *J. Phys. Chem. B* **2003**, 107, 8363–8371.
22. Gekko, K. In *Solution Properties of Polysaccharides*; Brant D. A., Ed.; ACS Symposium Series; Vol. 150, Washington, DC, 1981; pp 415–436.
23. Brant, D. A.; Liu, H.-S.; Zhu, Z. S. *Carbohydr. Res.* **1995**, 278, 11–26.
24. Liu, J. H.-Y.; Brant, D. A.; Kitamura, S.; Kajiwarra, K.; Mimura, M. *Macromolecules* **1999**, 32, 8611–8620.
25. Middendorf, H. D.; Di Cola, D.; Cavatorta, F.; Deriu, A.; Carlile, C. J. *Biophys. Chem.* **1994**, 53, 145–154.
26. Paradossi, G.; Di Bari, M. T.; Telling, M. T. F.; Turtu', A.; Cavalieri, F. *Physica B* **2001**, 301, 150–156.
27. Paradossi, G.; Cavalieri, F.; Chiessi, E.; Tellina, M. T. F. *J. Phys. Chem. B* **2003**, 107, 8363–8371.
28. Shepherd, P. D.; Kagunya, W. W.; Campbell, S. I.; Chapple, A. P.; Dryer, J. W.; Humphreys, R. J., et al. *Physica B* **1997**, 234–236, 914–916.
29. Texeira, J.; Bellisent-Funel, M.-C.; Chen, S. H.; Dianoux, A. J. *Phys. Rev. A* **1985**, 31, 1913–1917.
30. Singwi, K. S.; Sjölander, A. *Phys. Rev.* **1960**, 119, 863–871.
31. Chudley, G. T.; Elliott, R. J. *Proc. Phys. Soc.* **1961**, 77, 353–361.
32. Di Bari, M.; Deriu, A.; Albanese, G.; Cavatorta, F. *Chem. Phys.* **2003**, 292, 333–339.
33. Murase, N.; Watanabe, T. *Magn. Res. Med.* **1989**, 9, 1–7.
34. Watanabe, T.; Murase, N.; Staemmler, M.; Gersonde, K. *Magn. Res. Med.* **1992**, 27, 118–134.